Simulation of Ternary Organic Solar Cells to Study the Effects of Morphology and Material Properties on Power Output

Giovannone, Alex¹, Hershfield, Selman²

- 1. Department of Physics, The Ohio State University
- 2. Department of Physics, The University of Florida

Mentor: Selman Hershfield, Department of Physics

Abstract

Ternary organic solar cells were simulated as a 3D grid of resistors and photodiodes to study how a secondary acceptor as a third material affects the overall blend to optimize for power output. The voltage at zero current, $V_{\rm OC}$, of the donor and secondary acceptor interfaces should be at least that of the primary system. When the thickness and secondary acceptor conductivity are high, it is better for a secondary acceptor to stick to the main acceptor due to an asymmetry in current pathways. Otherwise, it is better to place the secondary acceptor next to the donor to increase the amount of donor: acceptor interfaces. These results are likely most applicable to the addition of fullerene acceptors into donor: non-fullerene acceptor blends, since their potential benefits come from an increased conductance and morphology as opposed to increasing the absorption spectra.

Keywords: Ternary organic solar cells, morphology, fullerene acceptors

Introduction

In recent years, exciting progress has been made in the universe of organic solar cells. Unlike traditional ones made of silicon, organic solar cells are constructed out of significantly cheaper materials that are flexible and often transparent (Duan 2019). These advantages have the potential of lowering the cost of renewable energy, making it more accessible to the average person.

However, for organic solar cells to compete, they need to be made more efficient. Two decades ago, they had power conversion efficiencies around 1%, microscopic in comparison to the 20% boasted by their silicon counterparts. After years of research, organic solar cells now achieve efficiencies around 16-18%. Most progress came from the introduction of improved

materials -- non-fullerene acceptors (NFAs) -- replacing their fullerene counterparts (Chang 2021). Nevertheless, the fullerene acceptors (FAs) have not been forgotten.

These old materials have found a new, unusual role in organic solar cells, but to see how, it is important to understand how solar cells typically work. When sunlight hits the active layer, it excites electrons into the conduction band. These electrons bind to the positively charged holes they left behind. This electron-hole pair is called an exciton. To harvest the energy stored in excitons, a solar cell uses the interaction of two materials: a donor and an acceptor. A chemical potential between the interfaces of the donor and acceptor materials creates an electrical field that can split excitons into unbound charged particles.

Since these free particles carry the electrical current, organic solar cells are designed to create as many of them as possible. By maximizing the surface area of interfaces between donor and acceptor, excitons are given more places to split apart. This is done by mixing and annealing the materials to form a structure called a bulk heterojunction, see figure 1 (Ray 2012). The discovery of non-fullerene materials fueled increases in power conversion efficiencies, keeping the bulk heterojunction design relatively the same (Li 2020).

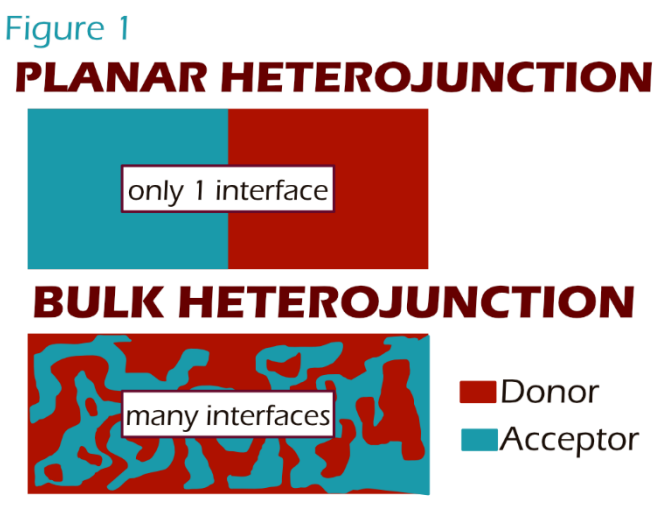


Figure 1. Planar Heterojunction vs Bulk Heterojunction. Traditional solar panels made of silicon utilize a planar heterojunction design. However, for organic solar cells, it is better to use a bulk heterojunction to maximize power output. Interfaces are the surfaces that donors and acceptors touch. By mixing the donor and acceptor, we create more interfaces to split apart excitons (Ray 2012). Throughout this paper, the interfaces in bulk heterojunctions were modeled as small planar heterojunctions.

However, over the past three years, a new design has emerged. It uses three materials as opposed to two in the active layer (Chang 2021). Given the straightforward picture of the two

material design, or binary organic solar cells, it may seem unclear where an additional material can contribute. These three material designs, or ternary organic solar cells, still have an acceptor and a donor, but they also have a 'helping material' in small quantities which tends to act as a secondary acceptor or secondary donor (Chang 2021). Through out this paper, we focus on adding a small amount of a secondary acceptor into the donor – main acceptor design. This makes our results most applicable to experiments which introduce a small amount of fullerene acceptors into donor: non-fullerene acceptor blends.

Binary organic solar cells with the older fullerene acceptors are worse than binary blends with non-fullerene acceptor on almost every metric. Subsequently, researchers moved away from using fullerene acceptors entirely. However, when a small amount of fullerene acceptors was added into a donor: non-fullerene active layer, power conversion efficiency improved to record high of 17.5% (Chang 2021). The literature suggests that this is due in part to higher electron mobility in fullerene acceptors and changes in active layer morphology (Gao 2020); however, there is still room for a more detailed and precise understanding of their benefit to ternary organic solar cells.

This paper aims to identify and understand the potential benefits of adding a secondary acceptor into the mix through computer simulation. We modeled ternary organic solar cells at various ratios and morphologies to understand how the sample's thickness, the secondary acceptor's conductivity, and the active layer's morphology impact the overall device performance. Our expectation, based on experimental results in literature, was that a secondary acceptor can improve the power produced by a ternary organic solar cell despite the donor: secondary acceptor interfaces producing less power than the donor: main acceptor ones.

Methods

The organic solar cells were modeled as a grid of cubes, each $10 \times 10 \times 10$ nm in size. Every cube was assigned a material: donor, main acceptor, or secondary acceptor. Neighboring cubes of the same material were connected with a resistor, which was determined by the material's conductivity. For the control, all three materials had the same conductivity $(5 \times 10^{-4} \frac{1}{\Omega m})$ and throughout the simulations, the conductivity of the main acceptor and donor did not change. Experiment shows the interface between two acceptors generates negligible power (Gao 2020), so we used the average resistance between the materials to connect primary acceptors to cubes of the secondary acceptor ones. Furthermore, the donor was connected to the top electrode with

resistors, and the main and secondary acceptors were connected to the bottom electrode with resistors.

Finally, donors and acceptors were connected with photodiodes. A modified version of the photodiode model proposed by Diantoro et. all was used (Diantoro 2018). Their work adds a shunt and series resistance term to the Shockley diode equation. Since our model already uses series resistance to connect cubes of the same type of material, we modeled the donor: acceptor interfaces by adding a shunt resistance term to the diode equation as so:

$$J = J_{s0}(e^{bV} - 1) - J_{sc} + G_{sh}(V - V_{oc}), \tag{1}$$

where V is the operating voltage (the independent variable), J is the output current density (dependent variable), and the rest of the parameters reflect the material properties: J_{sc} is the short circuit current density of the planar heterojunction (the y-intercept), V_{OC} is the voltage at zero current (the x-intercept), b is the ideality factor, J_{s0} is the dark saturation current density, and G_{sh} is the shunt resistance. For each donor: main acceptor interface, the parameters in the code that we vary are J_{sc} , V_{OC} , and G_{sh} . J_{s0} is determined by V_{OC} and J_{sc} , and the shunt resistance is multiplied by the difference of V and V_{OC} purely so that V_{OC} would correctly identify the voltage at zero current. An example J-V curve can be seen in Fig. 2.

The simulation ran in a custom MATLAB script, modified from previous research projects to support three material designs. It used an iterative process to simulate organic solar cell performance at a given voltage. The electrodes were set to this voltage difference and remained constant while the power converged. After making an initial guess for the voltages at every cube, the script checked to see if this guess was correct using Kirchoff's point law. It then updated every other cube's voltage using the voltage guesses around it. After updating the other half, the process was iterated. The specific numerical technique used is known as Gauss-Seidel, Simultaneous Over Relaxation (Isaacson 1988). Starting at V_{OC}, the script made 25 steps in electrode voltage difference to 0 and calculated the corresponding current densities in each step to 0.01% uncertainty. A *J-V* curve of each run was stored. Of note, it took an average of 10-15 minutes per *J-V* curve of computer time on the University of Florida's supercomputer.

Two interesting metrics can be taken from J-V curves to compare the performance of different devices. One is the maximum power. For a given J-V curve, the point of maximum

power was found by multiplying the voltages and their respective current densities together and taking the maximum. The other metric is the fill factor, conventionally defined to be the maximum power divided by J_pV_{OC} . To give a more intuitive definition, the fill factor is a number that ranges from 0.5 to 1 that states how rectangular the curve is. The higher the fill factor, the better the device will perform in practical applications.

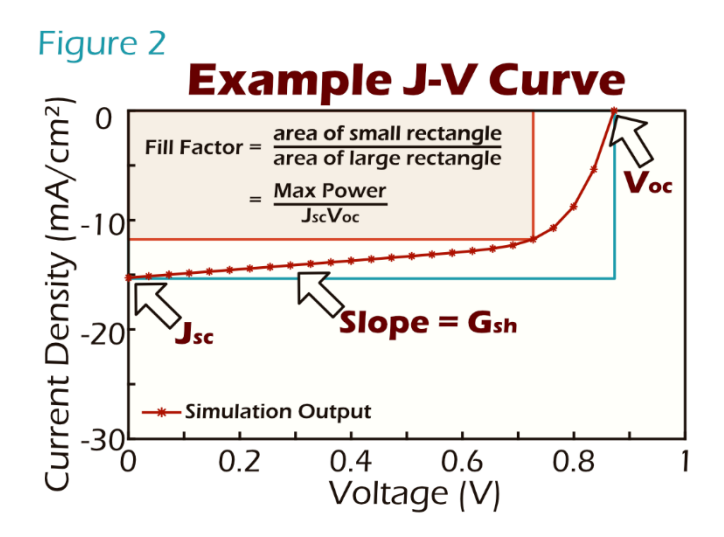


Figure 2. Example J-V Curve. For each sample, the simulation outputs a J-V curve. The y intercept is called the short circuit current density, Jsc. The x intercept is called the voltage at zero current, Voc. The slope after the curve is the shunt conductivity, Gsh. The fill factor determines how sharp the J-V curve bends.

To make the organic solar cell, a 550nm x 550nm wide 3D matrix with a variable height was created. It was then split into 121 columns that are 50nm x 50nm wide and as tall as the sample. Each column was assigned a material according to one of the templates shown in *Fig. 3*. These templates were designed to replicate the phase size observed in Raman spectroscopy images taken from previous experiments (Gao 2020, An 2020). These images show that the size of the material globs (>500nm) is significantly larger than the thickness of the sample (100-400nm), so the column approximation should be somewhat realistic. In literature, this large phase structure is associated with a longer length of annealing time (Ray 2012). From the Raman spectroscopy images, the secondary acceptor seems to have a tendency to stick to either the donor or main acceptor (Gao 2020, An 2020). To replicate this, the templates 1-8 have a glob of secondary acceptor fully embedded within a single material, and one at the interfaces. Template 9 represents the extreme case when the secondary material is just as common as the donor and

main acceptor. These templates allowed us to vary to ratio of secondary acceptor to other materials in discrete steps.

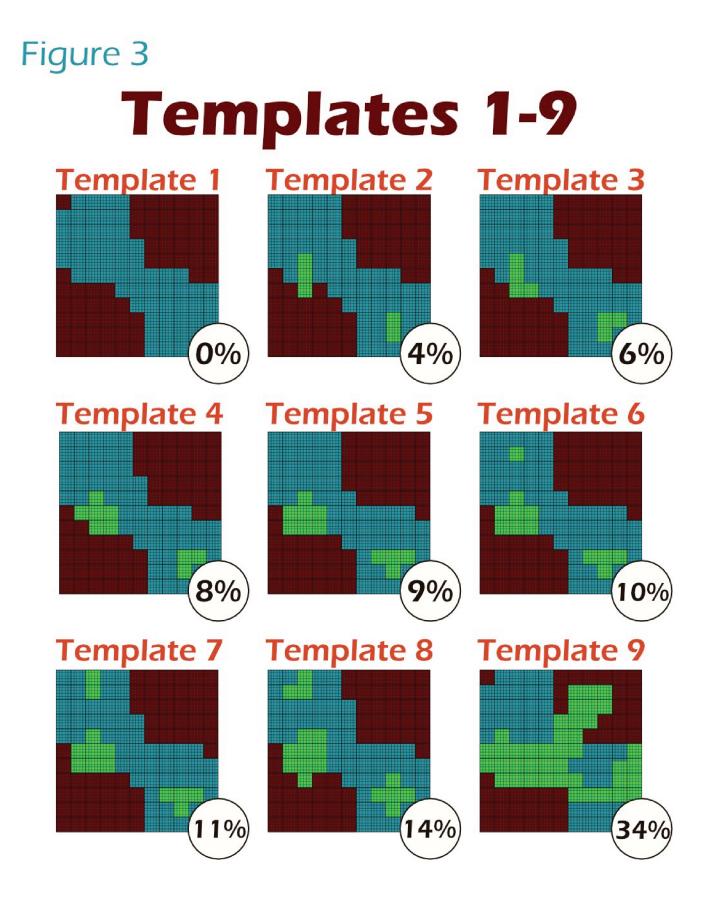


Figure 3. Computer Templates Used for Creating Sample Morphology. 50nm x 50nm single material columns were placed corresponding to each 5 x 5 square in a particular template. These templates have a constant ratio between the donor (red) and acceptor (blue), and an increasing ratio of secondary acceptor (from 0% to 34%). The ratio is printed in the circles. In each template, the light green squares represent vertical columns of secondary acceptor. The blue and red materials could be swapped to change whether the secondary acceptor sticks primarily to the donor or primary acceptor.

The literature cusses three different types of morphology (Huang 2018): the secondary acceptor embedded within the acceptor, the donor, and between the interface of the two. Semi realistic and simplistic templates were created to test the various cases as shown in *Fig. 4*.

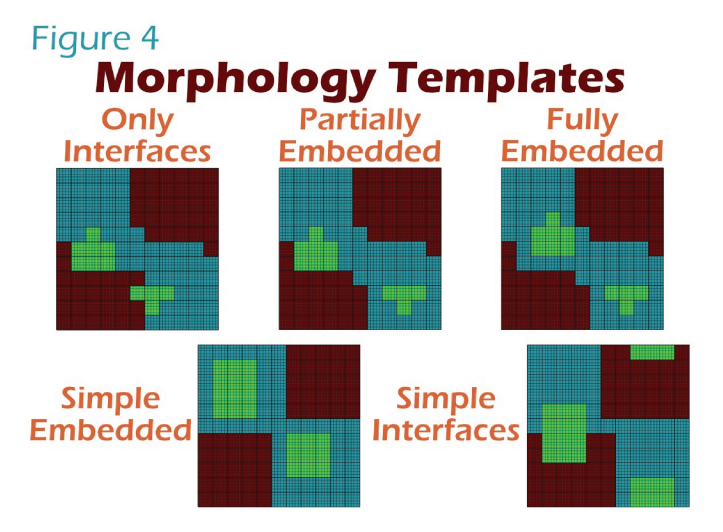


Figure 4. Computer Templates Used to Test Different types of Morphology. The top templates keep the ratio of secondary acceptor the same while changing the morphology of the sample. The bottom templates have been made much simpler to exaggerate the effect of the three types of morphology.

Using *template 1* in *Fig. 3*, parameters for the binary system were found by loosely fitting the *J-V* curve shapes found in experimental studies of PM6 : Y6 (Gao 2020, Yuan 2019). Since our model ignored quantum mechanical effects, quantitative accuracy was not achievable. Instead, we aimed for a qualitative understanding of experimental trends. Thus, the goal was not to match the exact values of any given experiment, but to match the trends along with the fill factor and short circuit current density. While most parameters could be easily read from experiment, the material conductivities were only accurate within an order of magnitude.

To create the control case of the donor: secondary acceptor blend, the J_{sc} parameter was halved, and the ideality factor was lowered in the photodiode equation. This lowered the maximum power and the fill factor of the donor – secondary acceptor blend, making it worse than the donor – main acceptor blend on all observable metrics. In real experiments, the maximum power of donor – fullerene acceptor blends are nearly half of that of their non-fullerene counterparts, making this a natural \Box ice (Gao 2020).

After this, one parameter was changed at a time to study how the properties of the secondary acceptor impact the ternary blend. The parameters used are listed in *Table 1*. Additionally, the *J-V* curves of each binary blend is shown in *Fig. 5*.

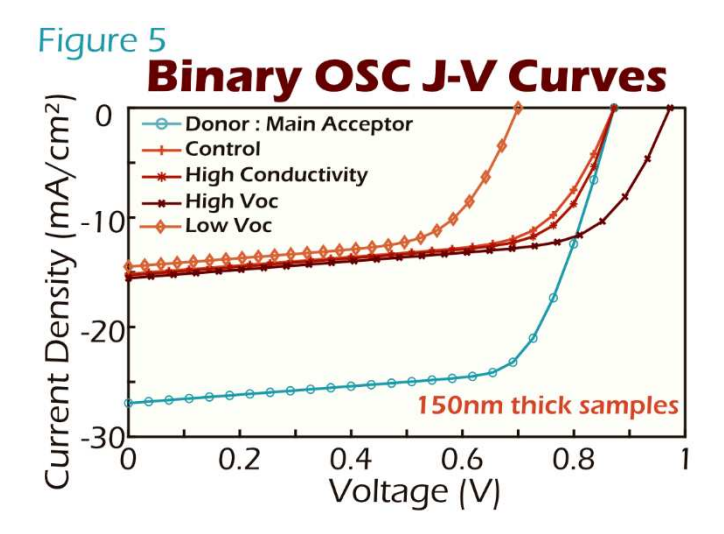


Figure 5. Binary OSC Curves For Each Set of Material Properties. The blue curve is the *J-V* curve of the primary binary system between the donor and the acceptor. The various red curves are the *J-V* curves of the donor and secondary acceptor binary system. The control has the same parameters as the primary system, except for a small short circuit current density and a lower ideality factor. The other secondary acceptor curves differ from the control by one parameter. Each of these tests were done with 150nm thick samples.

Binary System	Conductivity (1/ Ωm)	Voc (V)	$Jsc\ (mA/cm^2)$	b (1/V)	Shunt Conductivity
D:main acceptor	5 x 10 ⁻⁴	0.87	22	45	3.6 x 10 ⁻⁷
control	5 x 10 ⁻⁴	0.87	11	25	3.6×10^{-7}
High conductivity	5 x 10 ⁻³	0.87	11	25	3.6×10^{-7}
High Voc	5 x 10 ⁻⁴	0.97	11	25	3.6×10^{-7}
Low Voc	5 x 10 ⁻⁴	0.7	11	25	3.6 x 10 ⁻⁷

Table 1. The Simulation Parameters For Each Binary Curve Shown in Fig. 4. When the simulation mixed three materials, the parameters for the primary system and one of the secondary acceptor blends were used. The $V_{oc}s$ in the control and high V_{oc} cases were taken from literature (Gao 2020). The other parameters were fit to experiment.

Results and Discussion: The Lower Voc Dominates.

The effect of changing the relative V_{oc} values on the overall sample performance was studied. Some thicknesses are not included since they all show the same trends. The results are shown in *Fig.* 6.

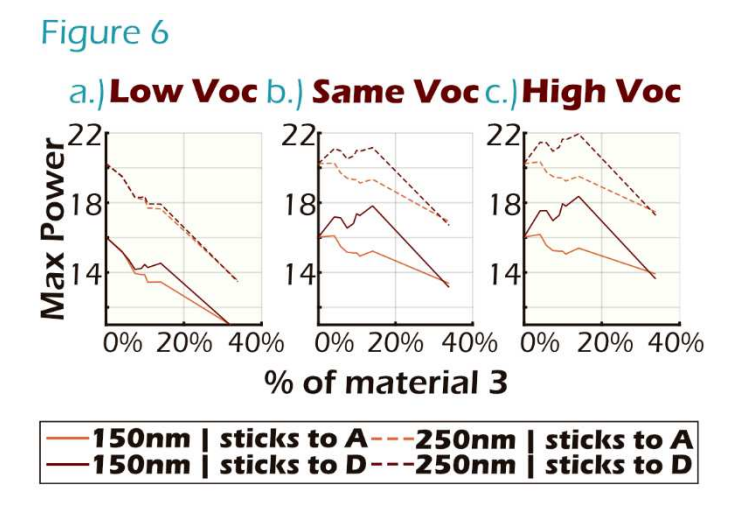


Figure 6. The Effect of Donor: Third Material V_{oc} Relative to Primary System V_{oc} . a.) the donor: secondary acceptor has a lower V_{oc} than the primary system. b.) The V_{oc} s are the same c.) the donor: secondary acceptor has a higher V_{oc} than the primary system. A lower V_{oc} is much more detrimental to a sample than a higher one is beneficial. The benefits of a higher conductance far out way those that come from a higher V_{oc} . This all implies that the lower V_{oc} dominates.

A low donor: secondary acceptor V_{oc} produces much less power than any other case; however, it doesn't appear that high V_{oc} produces much more than the case in which the blends share the same V_{oc} . This implies that the lower V_{oc} dominates the power output of a ternary blend. In every sample, when the system with the higher V_{oc} wants to perform its best (i.e. in high voltages), the other interfaces have effectively stopped functioning. The exponential term in eq 1 races off to extremely high values after passing V_{oc} , and with it, the ability to produce power. This trend is echoed in all of the runs, so the rest of this discussion will focus on understanding the interplay of secondary acceptor ratio, sample morphology, relative material conductivities, and sample thickness.

Results and Discussion: Ratio of Secondary Acceptor vs Power Output.

Using the templates in *Fig. 3*, the ratio of secondary acceptor to other materials was varied. For each ratio, the maximum power was computed for comparison. On the left hand side of *Fig.* 7, the secondary acceptor primarily sticks to the acceptor. On the right hand side, it primarily sticks to the donor. In the top control graphs, all of the materials have the same conductivities. In

the bottom, high conductivity graphs the conductivity of the secondary acceptor is increased by an order of magnitude.

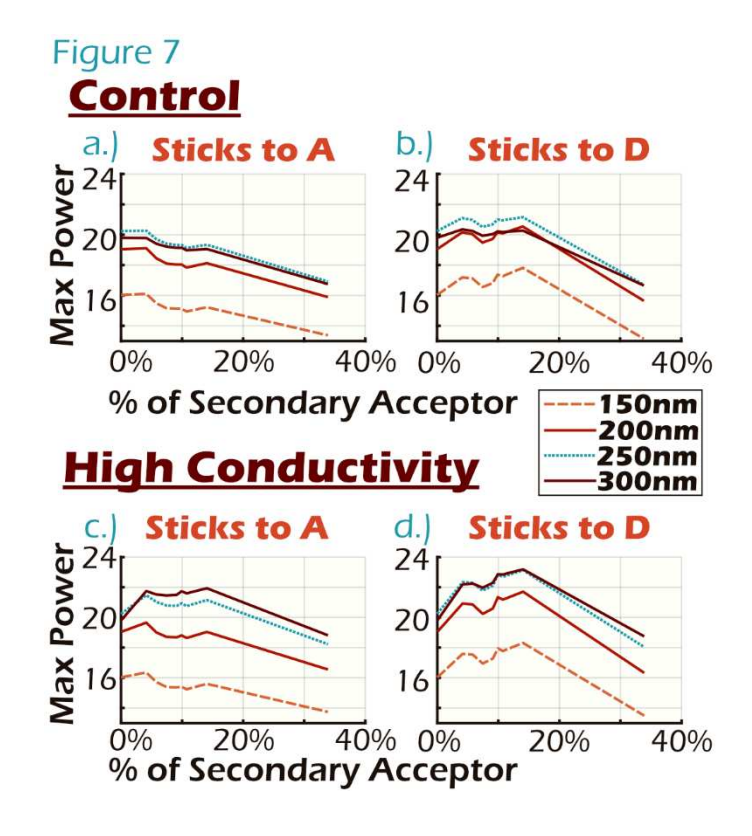


Figure 7. Ratio of Secondary acceptor vs Power Output with Morphology, Thickness, and Conductivity. In all graphs, the ratio was varied by using different templates in *Fig. 3.* a.) The donor: secondary acceptor system has the same parameters as the primary system except for a lower short circuit current density and lower ideality factor. The secondary acceptor has the tendency to stick to the main acceptor as opposed to the donor. b.) The same as *a*; however, the secondary acceptor sticks to the donor instead of the acceptor. c.) The same as *a*, except the conductivity of the secondary acceptor is an order of magnitude higher than the other materials. d.) The same as *b*, except with a higher secondary acceptor conductivity. *b-d* show the maximum power of a blend increases with a little addition of a secondary acceptor, but then decreases with a large addition.

There is an optimal thickness for any given blend, and this optimal thickness increases with an increasing conductivity. A thicker sample has more interfaces to generate power, but more series resistance to overcome. The balancing act of these conditions creates an optimal thickness. By increasing the conductivity, the series resistance decreases, thus raising the optimal thickness.

In the control case when the secondary acceptor sticks to the main acceptor (Fig. 7a), the maximum power never improves above its starting value. Even the slight bumps, caused by a

varying number of donor: acceptor interfaces, are not enough to raise maximum power above its initial value. This means that there is no benefit to adding in a secondary acceptor when its conductivity is the same and it sticks to the main acceptor. The only difference between the secondary and main acceptors in this case is that the donor: main acceptor produce twice as much power as the donor – secondary acceptor ones. Thus, by adding more secondary acceptor, the blend has less donor: main acceptor interfaces, which reduces the power output. This follows the intuition that adding a worse material makes the overall sample worse.

However, there is a significant power increase when the secondary acceptor sticks to the donor in the control case (*Fig. 7b*). This increase is caused by an increased number of donor: acceptor interfaces that do not come at the expense of the donor: main acceptor interfaces. This is further supported by data shown in figures 8 and 9. Intuitively, by sticking to the donor, the secondary acceptor can help the blend without getting in the way of the main acceptor.

With an increased conductivity in secondary acceptor, both samples generated more power with small amounts of secondary acceptor added but less power when too much of it is added, a trend supported by experiment (Chang 2021), and discussed more later.

Results and Discussion: Sample Morphology - Interfaces vs Embedding.

In Fig. 8, the ratio of secondary acceptor was kept fixed as the morphology changed, and its effect on the maximum power output of the ternary organic solar cell was studied.

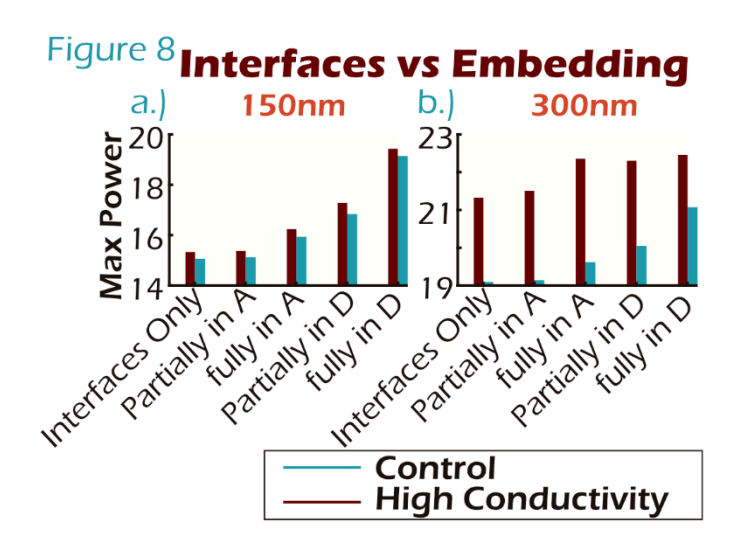


Figure 8. The Effect of Morphology on Power Output. a.) The samples tested were 150nm thick. b.) The samples tested were 300nm thick. maximum power of each blend were compared across different morphologies. This was done for the same material parameters presented in *Fig. 7*, where the secondary acceptor is in between the interfaces. In the limit of a high secondary to main acceptor ratio, we are left with the secondary acceptor: donor binary blend. This result is known to produce the least amount of power. Thus, it makes sense that the maximum power of decreases after too much secondary acceptor is added. Furthermore, the conductivity of secondary acceptor matters more in the thicker sample. In all cases but one it is better for the secondary acceptor to stick within the donor. The exception is when the sample is thick and the secondary acceptor is highly conductive, in which case it is better to stick to the acceptor.

In all cases, the 'interfaces only' template produces the least amount of power. The conductivity has a stronger impact on power generation in the thicker sample than the thinner one. Further, in most cases, the blend with the highest maximum power is the one where secondary acceptor is embedded fully within the donor. There is, however, one weird exception to this last pattern: the very thick high conductivity blend. In Fig. 8b, the highest maximum power comes the case when secondary acceptor is fully embedded within the main acceptor. To better understand these trends, the simple templates shown in Fig. 4 were ran. The results are viewable in Fig. 9.

Results and Discussion: Conductivity, Thickness, and Simple Morphology Structure.

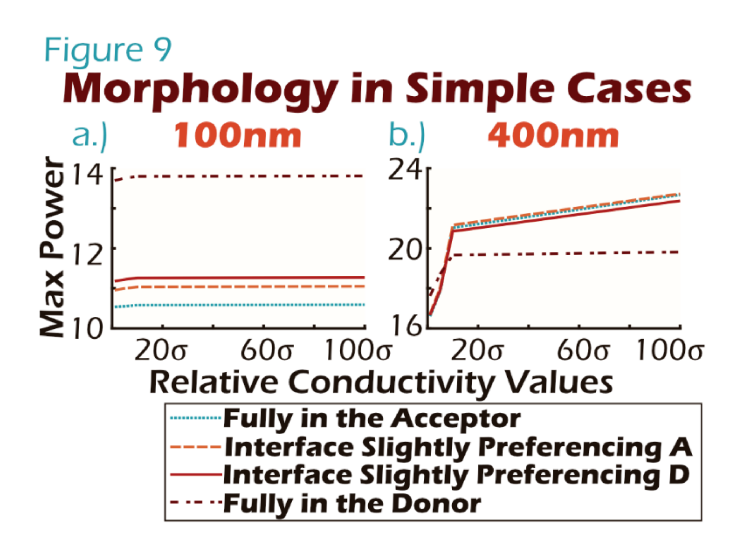


Figure 9. Varying Secondary acceptor Conductivity on The Simple Cases from Fig. 4. at 1σ the conductivities are the same between the materials. At 100σ , the conductivity of the secondary acceptor is 100 times larger than that of the main acceptor and donor. While being embedded within the donor is the most advantageous for low thickness or low conductivity, the opposite is true for high thickness and high conductivity.

Consider the low thickness case. Fully embedding within the donor increases maximum power output. Now consider the high thickness case. The conductivities matter more for the secondary acceptors that stick within the acceptor than for those that stick to the donor. Even though secondary acceptors that stick to the donor produce more power than their main acceptor counterparts, this relationship can flip if the sample is thick enough and the conductivity of the secondary acceptor is high enough.

When the conductivity is the same in secondary acceptor as the other materials, there is no difference between the 'fully embedded in the acceptor' case, and the main binary system. By placing the secondary acceptor inside the donor, the number of donor: acceptor interfaces has been increased, corresponding to the increase in power. Therefore, to maximize power, it is best to stick to the donor when the relative conductivities are similar or the thickness is small.

However, this design does not produce the highest maximum power: the design that does comes from a totally different mechanism. At large thicknesses, the power created by donor: secondary acceptor interfaces is mostly lost by the time it reaches the electrodes, so placing it inside the donor is not nearly as helpful as it was for lower thicknesses. When the sample is thick and the conductivity of secondary acceptor is high enough, the secondary acceptor is better at transporting charge than creating power, so its role in the ternary blend changes.

To understand how, it is helpful to consider the path of current in the sample. Since donor: acceptor interfaces are connected with photodiodes, current can only flow through an interface in one direction: acceptor → donor. It cannot go the other way around. Mathematically, photodiodes at the entrance and exit of the donor would point in opposite directions, effectively canceling out the current. This said, the strength of the donor: main acceptor photodiodes are different then the donor: secondary acceptor ones. This could allow the current to start in the main acceptor, enter the donor, and then enter the secondary acceptor. However, this path too is not allowed since the current would then have to reenter the donor before entering the electrode. Hence, there are a few possible paths for the current to traverse:

- 1. Primary Acceptor \rightarrow Donor
- **2.** Secondary acceptor \rightarrow Donor

- 3. Primary Acceptor \rightarrow Secondary acceptor \rightarrow Donor
- **4.** Secondary acceptor → Primary Acceptor → Donor

Of these paths, the most important is 4. On it, the charged particles can take advantage of an extremely conductive material, while also receiving the power boost from the primary interfaces. A similar path does not exist for when the secondary acceptor is within the donor, which is what causes the asymmetry in the data. When both the thickness and conductivity of secondary acceptor are high, these 'super highways' make it better to stick to the acceptor than it is to stick to the donor for power generation. Otherwise, it is best to stick to the donor and create more interfaces. The purpose of sticking within the main acceptor and donor flips if the secondary acceptor is instead a secondary donor.

Experiments show that when the fullerene acceptor $PC_{71}BM$ is added to a PM6: Y6 blend, it primarily sticks to the main acceptor, Y6, and increases the electron mobility, but decreases the hole mobility (Gao 2020). Our results show that the benefit in power output comes from Secondary acceptor \rightarrow Primary Acceptor \rightarrow Donor current pathways because of their high conductivity and high power output. When a secondary acceptor is added in small quantities, and sticks primarily to the acceptor, it can improve a thick ternary device if it has a significantly higher conductivity than the other materials, as can be seen in *Fig. 9b*. However, if too much is added, it will begin to get in the way of primary system's interfaces. As shown in *Fig. 8*, this is the worst place for the secondary acceptor to be in terms of device power output.

Conclusion

Computer simulations of ternary organic solar cells were performed on organic solar cells with a donor, main acceptor, and secondary acceptor to study the effect of a secondary acceptor's conductivity, the donor: secondary acceptor V_{oc} , the blend morphology, and the sample thickness on device performance. To optimize for power output, we found that a donor: secondary acceptor system should have a V_{oc} at least as large as the primary system. Furthermore, our results show that in thick samples, if the secondary acceptor has a significantly higher conductivity relative to the other materials, it is better for the secondary acceptor to stick to the acceptor. This benefit comes from Secondary Acceptor \rightarrow Primary Acceptor \rightarrow Donor current pathways. Otherwise, if the thickness is low or the conductivities are similar, it is better

for the secondary acceptor to stick to the donor. This is because of the increased donor: acceptor interfaces.

Our hope is that this work provides a small steppingstone in the greater goal of creating inexpensive solar energy. By understanding the role of a secondary acceptor in a ternary blend, better choices can be made in the future design of organic solar cells.

Acknowledgements

This work was supported by NSF grant DMR-1852138.

References

Gao, J., Wang, J., An, Q., Ma, X., Hu, Z., Xu, C., ... Zhang, F. (2020). Over 16.7% efficiency of ternary organic photovoltaics by employing extra PC 71 BM as morphology regulator. *Science China Chemistry*, 63(1), 83–91.

Duan, L., Yi, H., Wang, Z., Zhang, Y., Haque, F., Sang, B., ... Uddin, A. (2019). Semitransparent organic solar cells based on PffBT4T-2OD with a thick active layer and near neutral colour perception for window applications. *Sustainable Energy & Fuels*, *3*(9), 2456–2463.

Chang, L., Sheng, M., Duan, L., & Uddin, A. (2021). Ternary organic solar cells based on non-fullerene acceptors: A review. *Organic Electronics*, 106063.

Ray, B., & Alam, M. A. (2012). Random vs regularized OPV: Limits of performance gain of organic bulk heterojunction solar cells by morphology engineering. *Solar Energy Materials and Solar Cells*, 99, 204–212.

Li, S., Li, C.-Z., Shi, M., & Chen, H. (2020). New phase for organic solar cell research: emergence of Y-series electron acceptors and their perspectives. *ACS Energy Letters*, *5*(5), 1554–1567.

Markus, D., Thathit, S., Arif, H., Ahmad, T., Abdulloh, F., & Risa, S. (n.d.). Shockley's Equation Fit Analyses for Solar Cell Parameters from IV Curves. *International Journal of Photoenergy*, 2018, 7.

An, Q., Wang, J., Gao, W., Ma, X., Hu, Z., Gao, J., ... Others. (2020). Alloy-like ternary polymer solar cells with over 17.2% efficiency. *Science Bulletin*, 65(7), 538–545.

Huang, W., Cheng, P., Yang, Y., Li, G., & Yang, Y. (2018). High-performance organic bulk-heterojunction solar cells based on multiple-donor or multiple-acceptor components. *Advanced Materials*, 30(8), 1705706.

Yuan, J., Zhang, Y., Zhou, L., Zhang, G., Yip, H.-L., Lau, T.-K., ... Others. (2019). Single-junction organic solar cell with over 15% efficiency using fused-ring acceptor with electron-deficient core. *Joule*, *3*(4), 1140–1151.

Isaacson, E. (1988). *Numerical recipes: the art of scientific computing (william h. press, brian p. flannery, saul a. teukolsky, and william t. vetterling)*. Society for Industrial and Applied Mathematics.